Investigation of Fire Growth and Spread in a Model-Scale Railcar Using an Applied Approach

A. Kazemipour, M. Pourghasemi, H. Afshin[†] and B. Farhanieh

*Center of Excellence in Energy Conversion, School of Mechanical Engineering,
Sharif University of Technology, Iran, P.O. Box: 11155-9567*

†*Corresponding Author Email: afshin@sharif.edu (H. Afshin)*

ABSTRACT

Fire is a potential hazard in public transportation facilities such as subways or road tunnels due to its contribution to high number of deaths. To provide an insight into fire development behavior in tunnels which can serve as the basis for emergency ventilation design, model-scale railcar fire is explored numerically in this research. Fire growth and its spread are investigated by analyzing the HRR curve as the representative of fire behavior in different stages. Fire development has been predicted through a new approach using an Arrhenius-based pyrolysis model, established to predict the decomposition behavior of solid flammable materials exposed to heat flux. Using this approach, model-scale railcar fire curve is obtained and compared with experimental data. Reasonable agreement is achieved in two important stages of flashover and fully developed fire, confirming the accuracy of the presented approach. Moreover, effects of railcar material type, amount of available air, and surrounding are also discussed. Detailed illustrations of physical phenomena and flow structures have been provided and justified with experimental findings for better description of railcar fire behavior. The presented approach can be further used in other applications such as investigation of fire spread in a compartment, studying fire spread from a burning vehicle to another and reconstruction of fire incidents.

NOMENCLATURE

A_{ij}	pre-exponential factor (s^{-1})	$x_i, x^{(1)}, y, z$	Cartesian coordinate (m)
c_P	specific heat capacity (J kg^{-1} K^{-1})	$x^{(2)}$	number of carbon atoms in the fuel molecule
C_S	Smagorinsky constant	Y	species mass fraction (kg^{-1} kg^{-1})
D	diffusion coefficient (m^2 s^{-1})	Z	mixture fraction (kg^{-1} kg^{-1})
D^*	characteristic diameter (m)		
E_{ij}	activation energy (J mol^{-1})	δ_{ij}	Kronecker delta
g	gravitational acceleration (m s^{-2})	$\delta x, \delta y, \delta z$	cell size (m)
I_λ	radiation intensity at wavelength λ (W m^{-2})	Δ	width of grid filter (m)
k	conductivity (W m^{-1} K^{-1})	κ	local absorption coefficient (m^{-1})
MW	molecular weight (gr mol^{-1})	λ	wavelength (m)
P	pressure (Pa)	ρ	density (kg m^{-3})
Pr	Prandtl number	σ	Stefan–Boltzmann constant (W m^{-2} K^{-4})
P_m	background pressure (Pa)	τ	mixing time scale (s)
P^*	reduced pressure	τ_{ij}	stress tensor component (Pa)
Q	fire heat release rate	τ'_{ij}	sub-grid Reynolds stress (Pa)
q_c	heat release rate of chemical reaction (W m^{-3})	μ	dynamic viscosity (N s m^{-2})
q_r	radiative heat transfer (W m^{-3})	ν	stoichiometric coefficients in chemical reaction
R	universal gas constant (J mol^{-1} K^{-1})	*Superscripts*	

r_j	reaction rate (s^{-1})	-	filtered quantity
s	directional vector	~	Favre averaged quantity
s^*	stoichiometric ratio	*Subscripts*	
S_{ij}	strain tensor component (s^{-1})	∞	atmospheric conditions
Sc	Schmidt number	F	fuel
t	time (s)	O	oxidizer
T	temperature (K)	S$^{(1)}$	solid
u_i	velocity component (m s^{-1})	S$^{(2)}$	soot
x	cartesian coordinate vector (m)	t	turbulent

1. INTRODUCTION

Common methods to study fire and smoke spread are full-scale and reduced-scale experiments, numerical models and analytical methods. In full-scale experiments, passenger railcar fires are performed in both real tunnels and outdoors. The EUREKA 499 project (Haack, 1998), Second Benelux Tunnel fire experiments (Lemaire and Kenyon, 2006) and work by Peacock et al. (2004) are examples. Such tests are rare since they are expensive, time-consuming and complex to perform.

Reduced-scale experiments can be considered as an alternative, due to difficulties in performing full-scale tests. These experiments are often carried out by using Froude scaling technique and reveal main aspects of real situation with less cost and in a shorter time. Chow et al. (2010) investigated smoke movement in a tilted road tunnel using experiments in a 1:50 scaled tunnel. Hu et al. (2010) studied distribution of carbon monoxide and smoke temperature along the tunnel by series of experimental tests. Ingason (2007) investigated fire spread along with influencing factors in passenger railcars and measured heat release rate. He also applied simple theoretical equations used for estimating HRR in a compartment fire to predict peak HRR in a railcar fire. Most and Saulnier (2011) studied the behavior of a strongly contained wall fire in an enclosure during the post-flashover period in a laboratory scale experimental setup. They explored the fire intensity decay up to extinction of a wall fire due to lack of oxygen and the probability of the back-draft phenomenon

Although reduced-scale tests have fewer limitations than full-scale ones, obtained results cannot be completely converted to real fire results. This is due to lack of complete similarity between model and real samples. Furthermore, the theoretical methods are too restricted and only useful in simple geometries. These limitations along with major revolution in computer processing ability have persuaded the researchers to use numerical modeling as a powerful tool to study fire phenomena in recent years. As an early numerical work, Emmons's study (1979) can be noted in which he developed one of the first models for simulating fire in residential apartments. Nowadays, by increasing the accuracy and reliability of numerical models, advanced CFD models for simulating fires are being used in several fields such as smoke management, emergency ventilation systems performance, and material behavior exposed to fire.

Wang (2009) used CFD to predict soot and carbon monoxide production in a ventilated tunnel fire. Brahim et al. (2013) examined performance of two ventilation systems by comparing temperature distribution and pollutant stratification inside a road tunnel. Jia et al. (1999) studied pyrolysis process of non-charring materials and applied the results to predict fire spread within a compartment. Moghtaderi et al. (1997) developed a one-dimensional integral model for the transient pyrolysis of solid materials and estimated mass loss rate of materials exposed to heat flux.

The behavior of a railcar fire has high importance for the ventilation designer as it is the basis for design of smoke management systems in subways. System designer must be provided with information such as growth rate and peak heat release rate. It is also important to know about the effect of ventilation air on fire spread of and its intensification or retarding. Although many numerical researches have been performed on smoke movement, temperature distribution and toxic gases concentration, direct estimation of heat release rate and fire propagation in complicated fires by means of numerical simulation is still rare in literature. Zhang et al. (2007) numerically investigated fire spread and smoke movement in an underground car park. Fire source was designed by letting surface densities of the liquid fuel on top of the cars. Chiam (2005) simulated a metro train fire and estimated the heat release rate in different fire scenarios in subway tunnels. Hu et al (2012) investigated the fire spread in a passenger rail car compartment using an enhanced flame spread model. As observed by Peacock et al. (1999; 2002; 2004), heat release rate determines the emergency ventilation requirements; thus, it directly affects passenger train safety in fire incidents. It is thereby required to carry out more comprehensive research on fire spread and influencing parameters to ensure safety in real fires. To meet the goal, fire behavior of a railcar in different stages is predicted using a novel approach in this research. Arrhenius equation pyrolysis model is utilized through a new approach in order to estimate HRR and investigate the influence of certain parameters, such as interior material type and geometry of the openings. Physical assessment of flow structures and temperature and velocity distributions has been performed to visualize the results. Accuracy

of the presented approach is verified by experimental data on model-scale fire tests.

FDS 5.5.3 code is used in this study, due to its ability to well simulate the spread of fire-induced smoke. Mathematical models and CFD simulation parameters are described in Section 3.

1.1. Railcar Fire

To form a basis prior to discussions, a review of phenomena in railcar fires and more generally, compartment fires, have been provided. Enclosure fires can be represented by the temperature development in the compartment as shown in Fig. 1 for a typical geometry (Karlsson and Quintiere, 1999). It shows a typical time variation of temperature with five stages of uncontrolled fire growth. The stages include ignition, growth, flashover, fully developed fire and decay. Among the stages, flashover and fully developed stages are of the most importance.
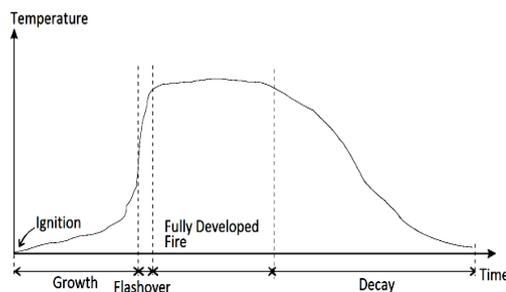
Fig.1. General description of uncontrolled compartment fire (Karlsson and Quintiere, 1999).

In the growth period, ignited fuel heats up the surrounding combustibles to a temperature in which they can release volatiles that can burn. The first minutes are usually spent in heating and not combustion. Flashover is a term used to describe a phenomenon where this locally burning fire transitions rapidly to a condition in which the whole compartment is involved in fire, causing a rapid increase in the size and intensity of fire. The ignition of all un-burnt combustibles, flame propagation through enclosure openings and rapid increase in temperature are the different phenomena associated with flashover. Gas temperatures of 500 to 600 ℃ have been generally reported during flashover (Karlsson and Quintiere, 1999; Walton and Thomas, 2002).

The second important stage is the post-flashover or fully developed fire. During this stage, the heat release rate (HRR) of the fire and the compartment temperature are the highest. In this period, the amount of air reaching the fire is insufficient for burning all the volatilevapors as the whole compartment openings have limited areas. The fire in such conditions is called ventilation-controlled, against fuel-controlled fire. The excess burning outside the compartment due to flames extension through the openings is the result of high temperature unburned fuel reaction with outside air. The average gas temperature in the enclosure during fully developed stage is very high, often in the range of 700 to 1200 ℃ depending on environment within the compartment (Karlssonand Quintiere, 1999; Walton and Thomas, 2002).

A similar curve to that shown in Fig.1 can be used for heat release rate. It is the rate at which energy is produced from combustion process. Similar to temperature, HRR increases very slowly in the pre-flashover and suddenly increases to post-flashover peak value in the flashover period. Therefore, either curve may totally represent the fire behavior.

The two described stages of flashover and fully developed fire have the highest importance in design of emergency ventilation systems. Ventilation engineers must know about the time to flashover and the peak fire intensity. Smoke extraction capacities depend directly on the peak HRR while passenger evacuation strategies rely on the flashover time.

This paper mainly emphasizes the peak fire intensity to help design efficient ventilation systems. The presented findings and procedures may also be used in design or pre-fabrication phase, prior to construction of railcar body, for reducing its fire propagation characteristics as the manufacturers must meet the standard requirements of high fire ratings.

2. PROPOSED METHOD DESCRIPTION

Predicting fire behavior of a railcar relies on solid combustibles' pyrolysis estimations. The problem of describing the pyrolysis of a solid material is to define the reaction or reactions converting virgin material to final products, and to obtain the kinetic parameters A, E, and n_s for each reaction (Vaari *et al.*, 2012). Therefore, specification of the kinetic parameters and reaction scheme in solid phase is vital to estimate production of gas volatiles and fire behavior. The mentioned parameters are not material properties but model constants which depend directly on the specified reaction scheme (Shen *et al.*, 2007; Matala *et al.*, 2008). Thereby, unique values are not found directly in literature.

As an alternative proposed method (Matala *et al.*, 2008), a reaction scheme is defined first and reliable experimental data, such as thermogravimetric analysis (TGA), on the decomposition process of the specified material are gathered. In the second stage, a satisfactory fit between the model and experimental data is obtained using numerical methods. Suitable kinematic parameters will be found via the described procedure.

Reaction schemes for wood and PVC are explored here as they will be used in this study. For wood pyrolysis, four reaction schemes, shown in Table 1, have been investigated (Matala *et al.*, 2008). The analysis indicated that for all reaction schemes except scheme 1, a reasonable fit between model

Table 1 Reaction schemes for wood

	Virgin Material	Intermediate Components		Final Products	
		Reaction rate	Component	Reaction rate	Component
Scheme 1:	Cellulose			k_1	Char + gas volatiles
	Lignin			k_2	Char + gas volatiles
	Hemicellulose			k_3	Char + gas volatiles
Scheme 2:	Solid			k_1	Char + gas volatiles
Scheme 3:	Solid 1			k_1	Char + gas volatiles
	Solid 2			k_2	Char + gas volatiles
Scheme 4:	Solid	k_1	Active	k_2	Char + gas volatiles
				k_3	Char + Gas volatiles

between model and experiment can be obtained. Scheme 4 is chosen as the wood decomposition reaction in this research.

PVC is an intumescent polymer which leaves char after pyrolysis (Shi and Chew, 2013). Therefore, in the current work, a single reaction scheme is used for PVC in which there is no intermediate component and virgin material converts to gas volatiles and char directly.

In this research, a new approach by using cone-calorimetry tests data is developed, as an extension to Hietaniemi et al. (2004) and Chiam (2005), in order to improve the accuracy of fire behavior estimations during a complex fire accident. The main basis of this approach is to predict the accurate behavior of solid flammable materials exposed to heat flux using a pyrolysis model based on Arrhenius equation. Upon this basis, the HRR fire curve may be estimated in different stages. The major focus is concentrated on the two important stages; flashover and fully developed fire. Obtained results may serve as feed data for safety and ventilation engineers. The proposed method is described by the following four steps:

1) Specifying flammable materials with high heats of combustion inside the railcar.

2) Conducting numerical simulation of cone calorimeter experiments for all materials specified in step 1 with determined solid phase reaction schemes.

3) Determination of kinetic parameters values in pyrolysis equation, Eq. (25), in order to obtain best fit to experimental HRR curves from cone calorimeter tests of step 2.

4) Simulating railcar fire using the parameters obtained in step 3.

3. NUMERICAL SIMULATION

3.1. CFD Tool

Version 5.5.3 of the Fire Dynamics Simulator (FDS) is used for numerical simulation in this study which is developed by the U.S. National Institute of Standards and Technology (NIST). FDS is widely used as a powerful numerical tool in fire and smoke spread related researches. Its reliability has been validated in many former fire related researches (Hu et al, 2010; Roh et al., 2007).

The core algorithm of the code is an explicit predictor-corrector scheme that is second order accurate in space and time. The partial derivatives of the conservation equations are discredited by finite difference method (FDM), and the solution is updated in time on a three-dimensional, rectilinear grid using an explicit second-order Runge-Kutta scheme. Thermal radiation is computed using a finite volume technique on the same grid as the flow solver. Staggered grid storage is incorporated (McGrattan et al., 2010).

3.2. Physical Phenomena and Mathematical Models

In order tostudydominant physical phenomena in a fire, governing equations for fluid flow, combustion in gas phase, decomposition of solid flammable materials and radiation should be solved simultaneously.

3.2.1 Fluid Flow

Filtering governing equations of continuity, momentum, energy and state in Cartesian coordinate system with filter width of Δusing Favre averaging yields(Poinsot and Veynante, 2001; McGrattan *et al*, 2010; Peters, 2000):

$$\frac{\partial \bar{\rho}}{\partial t} + \frac{\partial}{\partial x_i}(\bar{\rho}\tilde{u}_i) = 0 \quad (1)$$

$$\frac{\partial \bar{\rho}\tilde{u}_i}{\partial t} + \frac{\partial}{\partial x_j}(\bar{\rho}\tilde{u}_i\tilde{u}_j) + \frac{\partial \bar{P}}{\partial x_i} - \bar{\rho}g_i = $$
$$\frac{\partial}{\partial x_j}\left[\bar{\tau}_{ij} - \bar{\rho}(u_iu_j - \tilde{u}_i\tilde{u}_j)\right] \quad (2)$$

$$\frac{\partial(\bar{\rho}c_p\tilde{T})}{\partial t} + \frac{\partial}{\partial x_i}(\bar{\rho}c_p\tilde{u}_i\tilde{T}) = \frac{D\bar{P}}{Dt} + \frac{\partial}{\partial x_i}(k\frac{\partial \tilde{T}}{\partial x_i})$$
$$+ \frac{\partial}{\partial x_i}[-\bar{\rho}c_p(u_iT - \tilde{u}_i\tilde{T})] + \tilde{q}_c + \tilde{q}_r$$

(3)

$$\bar{P} = \bar{\rho} R \tilde{T} \sum_{\alpha} \frac{\tilde{Y}_{\alpha}}{MW_{\alpha}} \quad (4)$$

In order to model sub-grid Reynolds stress and turbulent heat diffusion, gradient diffusion conceptis employed:

$$\tau'_{ij} = \rho \left(u_i u_j - \tilde{u}_i \tilde{u}_j \right) = \frac{1}{3} \tau'_{kk} \delta_{ij} - 2\mu_t \tilde{S}_{ij} \quad (5)$$

$$\tilde{S}_{ij} = \frac{1}{2} \left(\frac{\partial \tilde{u}_i}{\partial x_j} + \frac{\partial \tilde{u}_j}{\partial x_i} \right) \quad (6)$$

$$\left(u_i T - \tilde{u}_i \tilde{T} \right) = \frac{\mu_t}{Pr_t} \frac{\partial \tilde{T}}{\partial x_i} \quad (7)$$

Turbulent Prandtl number is selected to be 0.5 (Kim et al. 2008). Smagorinsky model is used to calculate turbulent viscosity in momentum and energy equations (Smagorinsky, 1963).

$$\mu_t = \bar{\rho} \left(C_S \Delta \right)^2 \left| \tilde{S} \right| \quad (8)$$

$$\Delta = (\delta x \delta y \delta z)^{\frac{1}{3}} \quad (9)$$

The Smagorinsky constant, C_S,is set to be 0.2 (Kim *et al.* 2008; McGrattan *et al*, 2010).

A main assumption is made to simplify the governing equations of fluid flow. It is the low Mach number assumption as the resulting velocities from buoyant plume are low. However, high density variations are expected due to high temperature changes. The low Mach number denotes that the time scale associated with the fire growth and resultant fluid motion is usually long compared with the transit time of an acoustic signal. Therefore, flow equations may be characterized by a spatially uniform mean pressure (background pressure) with a spatially non-uniform portion of the pressure (reduced pressure). The former, being a function of time, appears in both the energy equation and the equation of state while the latter only appears in the momentum equation (Rehm and Baum, 1978; McGrattan *et al*., 2010).

$$P(\mathbf{x}, t) = P_m(z, t) + P^*(\mathbf{x}, t) \quad (10)$$

It must also be noted that molecular diffusion terms in momentum, energy and scalars may be neglected due to turbulent nature of flow. Applying the above mentioned assumption in Eqs. (1)-(4) forms the flow equations for thermally driven flows due to fires.

3.2.2 Gas Phase Combustion

Considering global reaction as below:

$$\nu_F [Fuel] + \nu_O [Oxidizer] \rightarrow [Products] \quad (11)$$
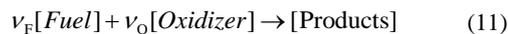
The mixture fraction, Z, is a conserved quantity defined as the (mass) fraction of the gas mixture that originates in the fuel stream:

$$Z = Y_F + \frac{W_F}{x W_{CO_2}} Y_{CO_2} + \frac{W_F}{x W_{CO}} Y_{CO} + \frac{W_F}{x W_S} Y_S \quad (12)$$

Sum of conservation equations for all species, along with the definition of mixture fraction yields a single conservation equation for Z (Zhang *et al*., 2007):

$$\frac{\partial}{\partial t} (\rho Z) + \frac{\partial}{\partial x_i} (\rho u_i Z) = \frac{\partial}{\partial x_i} (\rho D \frac{\partial Z}{\partial x_i}) \quad (13)$$

Using space filtering, Eq. (13)leads to:

$$\frac{\partial (\bar{\rho} \tilde{Z})}{\partial t} + \frac{\partial (\bar{\rho} \tilde{u}_i \tilde{Z})}{\partial x_i} = \frac{\partial}{\partial x_i} (\rho D \frac{\partial \tilde{Z}}{\partial x_i}) \\ - \frac{\partial}{\partial x_i} \left[\bar{\rho} (u_i Z - \tilde{u}_i \tilde{Z}) \right] \quad (14)$$

The last term in Eq. (14) is estimated using gradient diffusion concept wih turbulent Schmidt number of 0.5 (Kim *et al*, 2008).

In this research, a single-step reaction model is assumed as the global gas phase reaction with consideration of fuel with atoms C, H, O, N and M, shown in Eq. (15). Atom M accounts for other species in fuel chemical formula. The global reaction assumes that the fuel reacts with oxygen in one mixing-controlled step to form water vapor, carbon dioxide, soot, and carbon monoxide.

$$C_x H_y O_z N_a M_b + \nu_{O_2} O_2 \rightarrow \\ \nu_{H_2O} H_2O + \nu_{CO_2} CO_2 + \nu_{CO} CO + \nu_{Soot} Soot \\ + \nu_{N_2} N_2 + \nu_M M$$

$$(15)$$
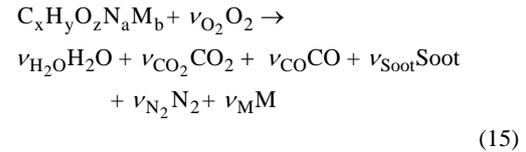
Stoichiometric coefficients are obtained using Eq. (16):

$$\nu_{N_2} = \frac{a}{2}$$

$$\nu_{O_2} = \nu_{CO_2} + \frac{\nu_{CO} + \nu_{H_2O} - z}{2}$$

$$\nu_{Soot} = \frac{MW_F}{MW_{Soot}} y_{Soot}$$

$$\nu_M = b$$

$$\nu_{H_2O} = \frac{y}{2} - X_H \nu_{Soot} \quad (16)$$

$$\nu_{CO} = \frac{MW_F}{MW_{CO}} y_{CO}$$

$$\nu_{CO_2} = x - \nu_{CO} - (1 - X_H) \nu_{Soot}$$

$$MW_{Soot} = X_H MW_H + (1 - X_H) MW_C$$

y_{CO} and $y_{Soot}$are carbon monoxide and soot yields existing in the post-flame.X_H is the atom fraction of hydrogen in the soot. Moreover, a, b, x and y are determined from the specification of the fuel molecule in Eq. (15)(Floyd and McGrattan, 2009).

For an under-ventilated fire, local extinction may occur due to oxygen depletion. The following correlation, between the oxygen mass fraction and the adiabatic temperature rise of the control volume,

is used to determine the possibility of combustion (Vaari *et al*, 2012):

$$Y_{O_2} = \frac{\overline{c}_p (T_{f,\lim} - T_m)}{\Delta H / r_{O_2}} \qquad (17)$$

In which, T_m is the temperature of the control volume and $\Delta H/r_{O2}$ is the heat release of fuel per 1 kg of oxygen consumption. Considering a critical flame temperature of 1700 K and an average specific heat of 1.2 kJ/kg.K (Senecal, 2005; McGrattan *et al*., 2010), approximate expression for the limiting oxygen mass fraction as a function of temperature will become:

$$Y_{O_2,\lim} = \frac{1.2 \times (1700 - T_m)}{13100} = 0.156$$
$$- 9.16 \times 10^{-5} T_m \qquad (18)$$

It can be inferred from Eq. (18) that, at 293 K, the limiting oxygen concentration (mass fraction) is 0.129, and falls linearly to zero at 1700 K. Based on SFPE handbook (Beyler, 2002), other researchers have reported limiting oxygen volume concentrations from 12 to 15 %. A value of 0.15 is considered in this research (McGrattan *et al*, 2010; Vaari *et al*., 2012).

A two-parameter mixture fraction, Z_1 and Z_2 such that $Z_1 + Z_2 = Z$, is used to calculate species concentrations capable of tracking fuel and products. Transport equations, similar to Eq. (14), are required for both Z_1, representing fuel, and Z_2, representing combustion products.

$$Z_1 = Y_F$$
$$Z_2 = \frac{MW_F}{xMW_{CO_2}} Y_{CO_2} + \frac{MW_F}{xMW_{CO}} Y_{CO} + \frac{MW_F}{xMW_{Soot}} Y_{Soot}$$
$$\qquad (19)$$

If combustion occurs, Z_1 converts to Z_2 representing the conversion of fuel to products. Mass fractions of species can be obtained by state relations after computing mixture fractions, Z_1 and Z_2, in the computational domain. State relation is the correlation between mixture fraction and mass fraction of each species. A detailed description of state relations along with the numerical approach are presented in Refs (Floyd and McGrattan, (2009); McGrattan *et al*., (2010).

The heat release rate from chemical reaction is computed in each cell:

$$q_c = \frac{\rho \min\left(Y_F, \nu_{O_2} Y_{O_2} \frac{MW_{O_2}}{MW_F}\right)}{\tau} \Delta H \qquad (20)$$

In which, τ is the mixing time scale:

$$\tau = \frac{C(\delta x \delta y \delta z)^{\frac{2}{3}}}{D_{LES}} \qquad (21)$$

The constant C is assumed to be 0.1 (Kim *et al*., 2008; McGrattan *et al*., 2010). ΔH in Eq.(20)is the

heat released in complete combustion of unit mass of fuel.

3.2.3 Radiation Model

Radiation has an important role in heating the walls and pyrolizing the combustibles. Radiation transport equation (RTE) has the following form for an absorbing, emitting and scattering medium (Siegel and Howell, 2002):

$$\mathbf{s}.\nabla I_\lambda(\mathbf{x},\mathbf{s}) = -\left[\kappa(\mathbf{x},\lambda) + \sigma_s(\mathbf{x},\lambda)\right] I_\lambda(\mathbf{x},\mathbf{s})$$
$$+ B(\mathbf{x},\lambda) + \frac{\sigma(\mathbf{x},\lambda)}{4\pi} \int_{4\pi} \Phi(\mathbf{s},\mathbf{s}^*) I_\lambda(\mathbf{x},\mathbf{s}^*) d\mathbf{s}^* \qquad (22)$$

It may be simplified assuming a non-scattering gas:

$$\mathbf{s}.\nabla I_\lambda(\mathbf{x},\mathbf{s}) = \kappa(\mathbf{x},\lambda)\left[I_b(\mathbf{x}) - I_\lambda(\mathbf{x},\mathbf{s})\right] \qquad (23)$$

Sdenotes direction vector and $I_b(x)$ is the source term given by the Planck black-body model, i.e. $I_b(x) = \sigma T^4/\pi$. The radiation transport equation must be solved by dividing the radiation spectrum into a relatively small number of bands. The current study does not consider the spectral dependence by assuming a gray medium with soot as the radiating gas. This is true as soot is the most important combustion product controlling the thermal radiation from the fire and hot smoke while its radiation spectrum is continuous.

3.2.4 Pyrolysis Model

Decomposition rate of a material in solid phase reactions is (McGrattan *et al*, 2010; Yang *et al*.,2011):

$$\frac{\partial Y_s}{\partial t} = -\sum_j r_j \qquad ; \qquad Y_s = (\frac{\rho_s}{\rho_{s0}}) \qquad (24)$$

The term r_j denotes the rate of j the reaction at temperature T_s which is calculated based on the Arrhenius model:

$$r_j = A_j Y_s^{n_{s,j}} \exp(-\frac{E_j}{RT_s}) \qquad (25)$$

A_j and E_j are the pre-exponential factor and activation energy, respectively. $n_{s,j}$ is the reaction order, $\rho_{s0}$is the initial density of the solid material layer and ρ_s denotes the mass of the remaining material (which is not decomposed) divided by layer's initial volume.

The assumption behind the pyrolysis model used in this research is that given a solid composing of N material components, the reaction rate converting component i to another substance (either an intermediate or a final product) can be written in Arrhenius form, Eq. (25) (Vaari *et al*, 2012).To calculate in-depth temperature at each combustible solid boundary, heat conduction is solved taking into account the solid decomposition reaction energy.

Table 2 Summary of simulation scenarios

Simulation scenario	Target	General description of scenario
1	Basic simulation for validation with experimental data	- 3.5 mm plywood as interior material - The door and all the windows are open, Fig. **2** - Fire occurs outdoors
2	Effect of interior material type	- 3.5 mm plywood is replaced by 7 mm PVC - Other situations are the same as scenario 1
3	Effect of ventilation	- Different arrangements of doors and windows are examined - Other situations are the same as scenario 1
4	Effect of surrounding	- Fire occurs in two tunnels with different cross-sections - Other situations are the same as scenario 1
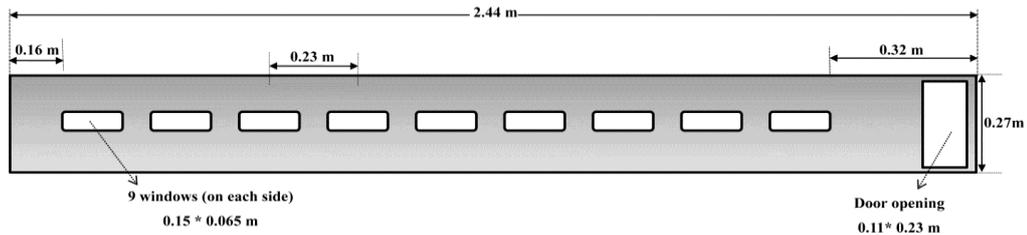
Fig. 2. Geometry of the railcar in fire simulation.

3.3. Description of Fire Scenarios

Using the proposed approach described in Section 2, fire spread in a railcar is studied and heat release rate is estimated in different cases. Four fire scenarios are simulated as described in Table 2. Case 1 is carried out based on Ingason's model-scale railcar fire test (2007) to verify the accuracy of the approach. Fig. **2** shows the railcar geometry in all simulation cases (except in scenario 3 with variations in openings arrangement), that is just similar to Ingason's setup.

The railcar ceiling and walls are covered by plywood and the seats are modeled with wood timbers in the first scenario. The door and all the windows of the railcar are open. In the second scenario, the effect of railcar interior material type on fire spread is investigated by changing the material from plywood in scenario 1 to PVC. In the third scenario, total area for air penetration through windows and doors is changed and the effect of air flow rate through the openings on fire spread and HRR is investigated. In the fourth scenario, railcar fire is simulated in two tunnels with different geometry shapes to study fires in confined spaces.

The body of model-scale railcar is constructed using noncombustible board. The ignition source consists of a 2×2×2 cm³ fiberboard cube placed on the floor, adjacent to the wall in front of the door. It is modeled with a constant HRR of 2 kW on the top surface of the cube and duration of 4 minutes.

3.4. Simulation Setup and Boundary Conditions

The computational domain for the fire in outdoor environment is a space with length of 3, width of 1.5 and height of 1.2 meters. The railcar is located in the middle of the domain. Pressure boundary condition is implemented for all boundaries meaning that air and smoke are free to enter or leave the domain. In case of fire simulation inside the tunnel, similar pressure boundary is used for both tunnel entrances while transient conductive heat transfer into the tunnel side-walls is considered. They heat up via radiation and give back some part the inflow heat via radiation and convection mechanisms. The ambient temperature and the initial temperature of all solid boundaries are considered to be 18 °C in all cases. Railcar body is considered to form wall boundaries with no slip condition and is heated up via conduction. It is composed of combustible sections that burn and non-combustible sections that only get warm. The boundary condition for the fire source is mass inlet of the gas fuel. The mass flow is adjusted for the required power.

One-dimensional heat conduction is solved to calculate in-depth temperature at each solid boundary with a uniform solid mesh grid. The heat conduction is solved each time step.

The chemical formulae of gas volatiles for wood and PVC used in gas phase combustion, Eq. (15), are considered as $C_{3.4}H_{6.2}O_{2.5}$ and C_2H_3Cl, respectively (Hietaniemi *et al.* 2004). Furthermore, 12000 and 13000 kJ per kilogram of oxygen are assumed as heats of combustion for wood and PVC (Hietaniemi *et al.*, 2004).The railcar fire is oxygen-lean; therefore, post-flame soot yield is supposed to be 0.12 for wood combustion and 0.17 in case of PVC. Carbon monoxide yield is specified to be 0.05 for both

materials (Hietaniemi *et al.*, 2004; Tewarson, 2002).

In order to discretize the radiation transport equation, 100 solid angles are used (Ferng and Lin, 2010; Lin *et al.*, 2009).

The domain is longitudinally separated into three parts in the tunnel fire study. Mesh cells are finer in the section that contains the railcar and are coarser in the two other sections. Uniform grid is used in case of outdoor fire.

3.5. Grid Study

A characteristic length named characteristic fire diameter (D^*) is defined (McGrattan *et al.*, 1998) to check the ability of grid resolution to capture main aspects of fire behavior:

$$D^* = \left(\frac{Q}{\rho_0 T_0 c_p \sqrt{g}} \right)^{2/5} \quad (26)$$

It is recommended to sweep this characteristic length with four to sixteen mesh cells ($D^*/\delta x$) near fire source (McGrattan *et al.*, 1998). As the HRR is not known in advance and varies with time due to fire spread throughout the railcar, and also solid phase reactions are involved, grid sensitivity test is performed in order to capture acceptable resolution of flow field. Three outdoor fires imulations with uniform grid of different cell sizes are carried out to check the sensitivity of the results to grid distribution. It must be noted that the geometry of the railcar is modified against Fig. **2** so all the dimensions are multiples of coarsest mesh cell. This prevents any deformation in the geometry between different grids.

The fire curve or variations of HRR is selected for mesh study procedure as it can well represent the physical phenomena within a railcar fire. The results from the three grids are shown in Fig. **3**. The medium grid may be chosen as the optimal case.

4. RESULTS AND DISCUSSION

4.1. Basic Simulation

Calculated heat release rate for the railcar fire is shown in Fig. **4** and compared to experimental results of Ingason (2007). The result in major parts such as fire growth, flashover and post-flashover regions follows these experimental data. However, there is a mismatch in fire decay stage. In order to investigate the reason, cone calorimeter test for plywood is explored in more detail.

Fig. **5** shows the heat release rate of plywood in cone calorimetry and the best-fitted curve obtained. The large st deviation from experimental data occurs in fire decay stage. The fire stops sooner in present work compared to actual conditions. Charring process and smoldering fire which is responsible for late extinction of fire is not captured well in the numerical model. Therefore, some decomposition mechanisms of flammable materials

inside the railcar are not estimated exactly and these results in the mismatch observed in fire decay stage of railcar fire.
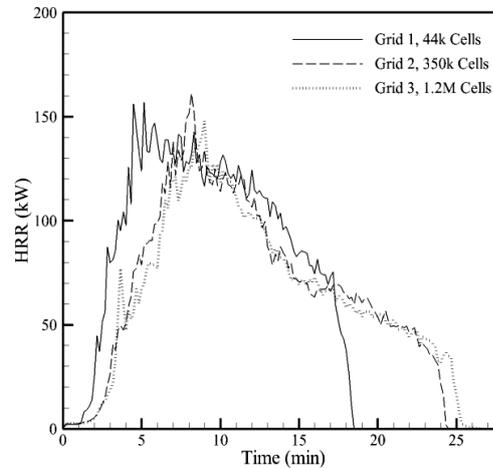
Fig. 3. Fire curve for three different grids.
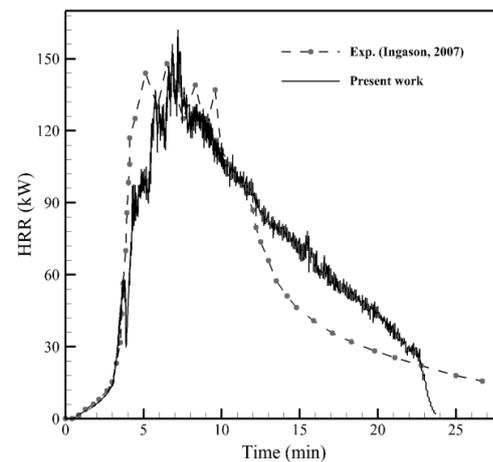
Fig. 4. Calculated and measured heat release rates in first railcar fire scenario.

Revisiting Fig. **4**, it can be noted that the total energy released from two railcar fire tests are similar. This is done by integrating the curve over time to calculate a value of about 95 MJ. Therefore, the proposed reaction mechanisms consume the flammable materials faster which leads to earlier extinction. As mentioned before, the flashover and fully developed stages are of highest importance. Thus, efforts are focused to capture physics in these stages and satisfactory agreements are achieved.

4.2. Physical Discussions

The HRR fire curve contains many physical phenomena and can well represent the behavior of a compartment fire. Different stages of railcar fire according to this curve are deeply investigated in this section.
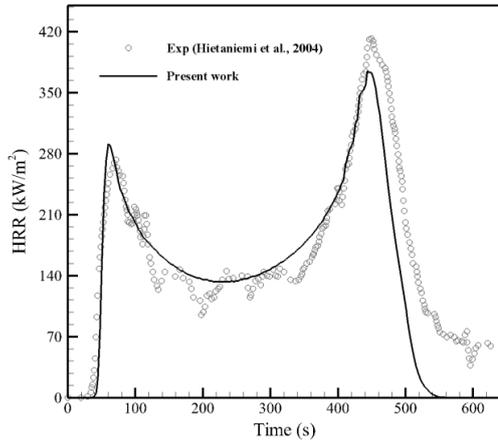
Fig. 5. Experimental and best fitted numerical heat release rates in plywood cone calorimeter test.

The first examination is the onset of flashover. As previously described, flashover is a transition from a local fire to a fully developed fire. As it can be seen in fire curve of Fig. **4**, flashover occurs between minutes 3.5 to 5 as HRR increases rapidly in a short time. The rate of fire growth is slow before this time. In this regard, temperature contours are plotted in the first five minutes from ignition. Results are presented in Fig. **6**. Temperature contours are averages of ten seconds. As it can be seen, no significant temperature increase is observed within the first three minutes except that the smoke has filled a larger portion of the enclosure. However, around minute 4, temperature starts to rise significantly. At minute 5, temperature in almost all of the compartment space has increased to about 400ºC and above. As explained before, the dominant transfer phenomena in the beginning of a fire is thermal radiation. The environment is heated gradually and releases gas volatiles until their flow rate is enough to support combustion. In this moment, the fire propagates rapidly to the whole compartment.

Air entrainment through openings plays an important role in compartment fire development as such fires are generally ventilation-controlled. Openings allow for fresh air entrance and smoke exit to facilitate the combustion process. Fig. **7** presents the time variation of inflow and outflow through openings, that is, the single door and all the 18 windows as seen in Fig. **2**, for the railcar fire. As can be seen, windows mainly contribute to outflow of smoke rather than inflow of fresh air while the door has similar amounts of in and out flows. The windows handle a high portion of outgoing smoke, about five times the share of the door.

This can be attributed to the fact that density variations inside the hot enclosure induce pressure gradients in the direction of gravity. Windows being located in higher levels, mainly contribute to smoke outflow. It must be mentioned that the windows have a total area of about 6 times the

area of the door in the railcar geometry complying with the relative shares of the windows and the doors in outflow as previously stated. Also, summation of the inflows and outflows results in a net mass flow out of the compartment. This can be justified by the fact that enclosure heating pushes some air outwards due to density reductions. Fig. **7** also describes the flashover phenomenon. As can be seen, a sudden increase in smoke outflow occurs in about minute 4. This is due to flashover occurrence which yields to sudden temperature increase and a high production rate of hot smoke. Above observations comply with descriptions provided by Karlsson and Quintiere (1999). Quantitative discussion on air entrainment is presented in Section 4.4.
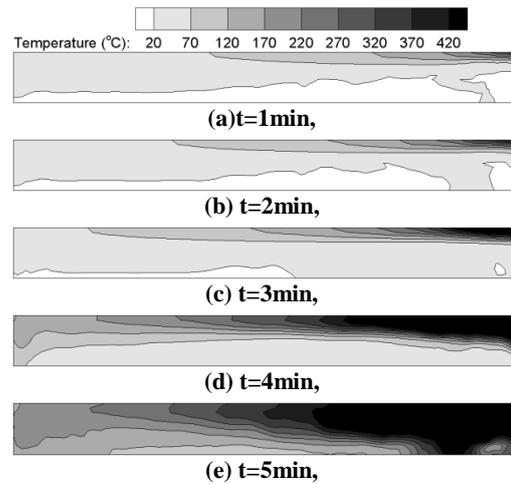
Fig. 6. Development of fire from ignition time. Temperature contours are ten second averages.
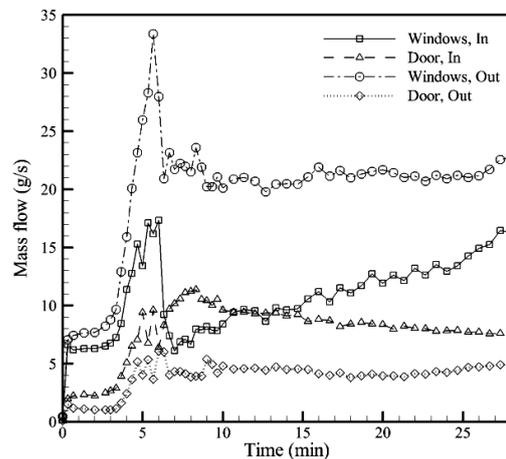
Fig. 7. Time variation of mass flow exchange through railcar openings.

In order to shed light on air entrainment phenomena, plots of flow vectors in railcar section at locations of the door and a pair of windows are shown in Fig. **8**. The plots support the above observations. The door serves as both fresh air intake and smoke exit. It must be noted that for a similar mass flow rate, flow velocity for smoke is about twice the fresh air due to elevated

temperatures. The vector plots in Fig. **8** are 30 second averages in the fully developed stage of fire.
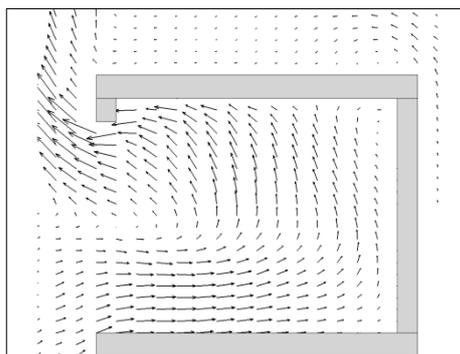
(a)
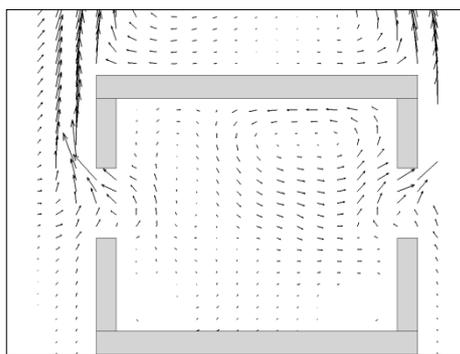
(b)

Fig. 8. Slice vectors showing the inflow of fresh air and outflow of smoke in location of (a) the door, and (b) one of the windows. Scale of vectors in (b) is twice the vectors in (a).

The final interesting point is the excess burning outside the compartment. As previously described, this happens because some unburned volatiles exit the compartment while mixed with outgoing combustion products. They catch fire as they reach oxygen at onset of discharge through the openings. This phenomenon is depicted Fig. **9** which presents a snapshot of temperature contour in the fully developed stage. High temperatures, about 500 °C, are observed in the window discharge showing the flame existence. Similar findings are reported in other researches (Ingason, 2007; Hammarström *et al*., 2008; Hietaniemi *et al*., 2004).

4.3. Effect of Interior Material Type

The influence of flammable material type on the railcar fire has been investigated in this section. For this purpose, plywood is replaced by PVC and the heat release rate curves are compared. Fig. **10** shows the result.

According to the figure, the fully developed stages of the two curves are similar, even though the types of flammable materials and the corresponding cone calorimetry behaviors are different. Maximum heat release rate of PVC in cone calorimeter test is approximately 145 kW/m^2 compared with 420 kW/m^2 for plywood (NIST, 1999; Chow *et al*., 2004; Hietaniemi *et al*., 2004). This is similar to the

result obtained by Ingason (2007) that observed the same peak HRR in his railcar fire tests with two different internal materials (3.5 mm plywood and 13 mm corrugated cardboard).
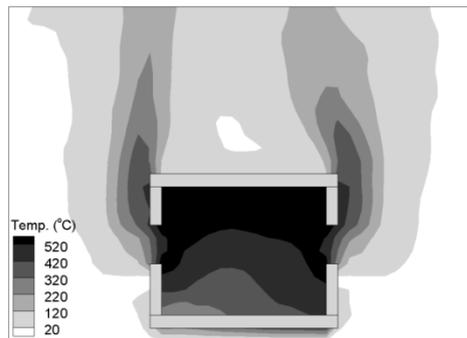
Fig. 9. Temperature contour in a transverse section of the railcar in location of one pair of windows.
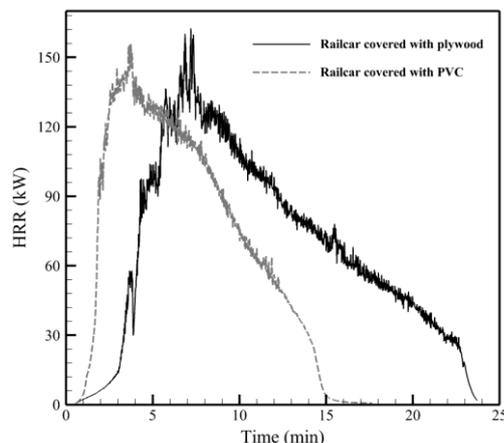
Fig. 10. Calculated heat release rate in railcar fire with different interior material types (PVC versus plywood).

The reason can be associated with the air entrainment and ventilation conditions. As stated before, railcar fires are controlled by the ventilation rate as the amount of supply air reaching the fire is insufficient for burning all the fuels. Therefore, limited ventilation does not support large fires despite using different combustibles. The material type only affects the growth and flashover stages. PVC has lower fire ratings compared to wood; therefore, the PVC railcar catches fire more easily and fully develops in a shorter time.

4.4. Effect of Ventilation on HRR

In previous sections, ventilation has been proved to be a key parameter affecting compartment fire behavior. Influence of ventilation availability on railcar fires is investigated in this section. Based on Rocket's research (1976), air mass flow rate through the openings for ventilation-controlled fires near the flashover and post-flashover regions, is proportional to ventilation factor, Eq. (27):

$$\dot{m}_{air} \propto A_0 \sqrt{H_0} \qquad (27)$$

Table 3 Railcar ventilation conditions and the resulting fire intensities

Case	Ventilation factor, Ψ (m²)	$Q = 1500 A_0 \sqrt{H_0}$ (kW)	Maximum observed HRR (kW)	Correction factor, η
1	0.027	40.6	50.4	1.24
2	0.037	55.5	87.0	1.57
3	0.042	62.9	106	1.69
4	0.057	85.3	161	1.89
5	0.073	110	239	2.18
6	0.083	125	292	2.34
7	0.093	140	346	2.48

H_0 and A_0 are height and area of openings, respectively. The effect of opening height as mentioned previously appears in this correlation quantitatively.

By considering the mass fraction of oxygen in air as 0.23, and heat release per unit mass of consumed oxygen as 13000 kJ, the maximum HRR in ventilation-controlled fires is obtained (Ingason, 2007):

$$\dot{Q}_{max} \approx \eta 1500 A_0 \sqrt{H_0} \quad (28)$$

η is the correction factor responsible for additional fuel burning outside of the openings.

To study the effect of excess air reaching the fire due to failure of windows, correction factors in seven different arrangements of openings are estimated. The railcar geometry is similar to the first scenario, with different total area of openings. Table 3 shows the summery of seven simulations including the HRR estimation from Eq. (28) and the values of HRR and correction factor from railcar fire simulations.

As seen in Table 3, correction factor grows as ventilation factor increases. This is similar to the result obtained by Bullen and Thomas (1979). It can also be deduced that, the peak HRR in this railcar fire drastically depends on the amount of ventilation; i.e., with a higher rate than estimated by Eq. (28).

To more deeply investigate the air entrainment effect, ventilation factors are normalized by the maximum possible ventilation factor for the railcar geometry in Fig. **2**. Correction factor variations with normalized ventilation factor along with the best fitted curve are shown in Fig.11. A regression may be proposed from the plot as follows:

$$\eta = (1640)\Psi^3 - (444)\Psi^2 + (50.7)\Psi - 0.0532 \quad (29)$$

In which, Ψ is the normalized ventilation factor.

The correction factor for fire in a railcar, with similar geometry as Fig. **2**, can be obtained from Eq. (29). In this way, fully developed fire characteristics can be estimated without any further simulations or experiments. Further, the similarity correlations (Ingason, 2007) may be used to upscale

the results in order to predict full scale fire conditions.

Fig.11 also shows the three correction factors obtained by Ingason (2007) in his model-scale railcar fire test. The acceptable agreement confirms the accuracy of presented correlation to predict fully developed peak HRR in ventilation-controlled fires for a railcar of similar geometry.
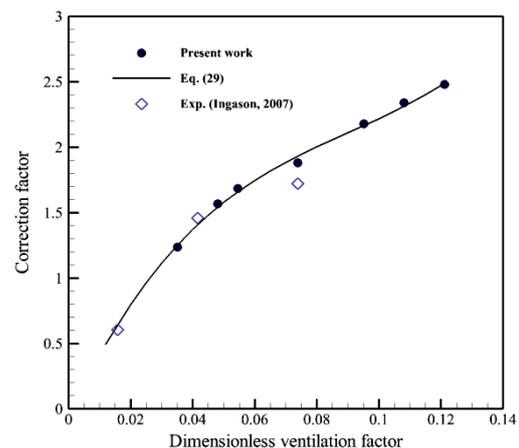
Fig.11. Correction factor based on dimension lessventilation factor.

4.5. Fire in Tunnels

In this section, simulation of railcar fire inside tunnels with natural ventilation is carried out. The railcar geometry and its interior flammable materials are just the same as the first scenario. In order to study the effect of tunnel geometry on HRR, simulations are conducted in two tunnels with different cross-sections shown in Fig.12. In both simulations, the tunnel length is 8 m.

Calculated HRR curves are shown in Fig.13. Comparison of tunnel A's fire behavior with the outdoor fire, Fig. **4**, reveals that the initial rate of fire growth and flashover are the same. But the fully developed stages are dissimilar and the peak HRR for the case of fire inside the tunnel is lower than that of the outside fire. The reason lies behind the fact that smoke and hot gases occupy the upper parts of the tunnel as they travel longitudinally under ceiling in order to exit the tunnel. For the low height tunnel, this limits the ventilation conditions

of the railcar fire. It must be noted that in naturally ventilated tunnels, opposite flows of upper smoke layer and lower fresh air layer occur leading to significant mixing at the interface. For the same reason, the fuel-controlled initial stages of fire are therefore for both conditions.
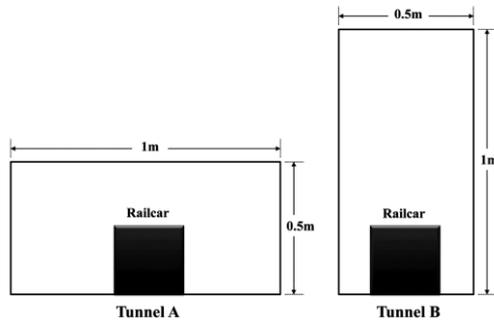
Fig.12. Cross sections of the two tunnels used in simulations.
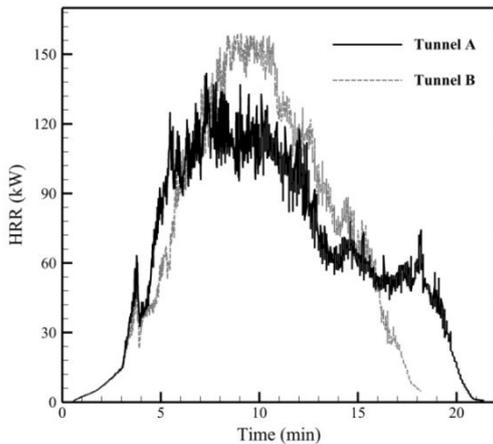
Fig.13. Calculated heat release rate of railcar fire inside tunnel.

Considering tunnel entrances as openings, the amount of fresh air reaching the fire is a function of entrances geometry. As mentioned in the previous section, height and area are the two key parameters. Therefore, lower peak HRR is expected for tunnel A with lower height compared to tunnel B. This is in accordance with the fully developed stages of the tunnel fires as seen in Fig.13.

5. CONCLUSION

In this research, a railcar fire in model-scale was studied numerically and the affecting parameters were investigated. The time variation of heat release rate, or fire curve, was mainly explored in this regard as it contains full description of railcar fire conditions in all stages including flashover and fully developed fire. To predict the fire behavior, the concept of materials effective kinetic parameters was developed to be used in Arrhenius equation pyrolysis model, in order to capture the accurate decomposition behavior of solid flammable materials exposed to heat flux. Obtained kinetic parameters for any single material, found via small-scale tests, were incorporated into the full railcar

fire with complex geometry. Acceptable agreement with experimental data in fire growth, flashover and fully developed stages, verified the ability of the presented approach, although it predicted a faster fire decay stage compared to experiment. Also, various illustrations of flow structures along with justification with experimental findings were provided to better percept the physical phenomena during a railcar fire.

Simulation results showed that the railcar fires, both inside and outside the tunnel, were ventilation-controlled in the fully developed stage. Therefore, the peak HRR was a strong function of air supplied to the fire source from the openings and did not depend considerably on the interior flammable materials type. The type of combustible material was however important in initial fuel-controlled stages and affected the time to flashover significantly. It was also observed that the geometry of tunnel entrances played a significant role in fire spread and determined the maximum heat release rate.

Since the presented approach can well estimate the initiation of fire and its growth, it can be found useful in further applications. These applications include studying fire spread in a compartment, spread mechanism from a burning vehicle to another, reconstruction of fire incidents and estimation of critical ventilation velocity in a real tunnel railcar fire. Also, it must be mentioned that major efforts in current research were focused on flashover and fully developed stages as the basis for design of emergency ventilation; improvement of the method for better estimation of fire behavior in decay stage may be considered as a developing future work.

REFERENCES

Beyler, C. L. (2002). *Flammability Limits of Premixed and Diffusion Flames*. in SFPE Handbook of Fire Protection Engineering, handbook of fire protection engineering, 3rdedition. Quincy, Massachusetts, National Fire Protection Association.

Brahim, K., B. Mourad, E. C. Afif and B. Ali (2013). Control of Smoke Flow in a Tunnel. *Journal of Applied Fluid Mechanics 6(1), 49-60*.

Bullen, M. and P. Thomas (1979). Compartment fires with non-cellulosic fuels. *Symposium (International) on Combustion, Elsevier*.

Chiam, B. H. (2005). *Numerical simulation of a metro train fire*. Christchurch, University of Canterbury. M.Sc. Thesis.

Chow, C. L., W. K. Chow, N. K. Fong, Z. Jiang and S. S. Han (2004). Assessing fire behavior of common building materials with a cone calorimeter. *International Journal on Architectural Science 5(4), 91-98.*

Chow, W. K., K. Y. Wong. and W. Y. Chung (2010). Longitudinal ventilation for smoke

control in a tilted tunnel by scale modeling. *Tunnelling and Underground Space Technology 25(2); 122-128.*

Emmons, H. W. (1979). The prediction of fires in buildings. *Symposium (International) on Combustion, Elsevier.*

Ferng, Y. and C. Lin (2010). Investigation of appropriate mesh size and solid angle number for CFD simulating the characteristics of pool fires with experiments assessment. *Nuclear Engineering and Design 240 (4), 816-822.*

Floyd, J. and K. McGrattan (2009). Extending the mixture fraction concept to address under-ventilated fires. *Fire Safety Journal 44(3), 291-300.*

Haack, A. (1998). Fire protection in traffic tunnels: general aspects and results of the EUREKA project. *Tunnelling and Underground Space Technology 13(4), 377-381.*

Hammarström, R., J. Axelsson, M. Försth, P. Johansson and B. Sundström (2008). *Bus fire safety.* SP report 41, SP Technical Research Institute of Sweden.

Hietaniemi, J., S. Hostikka and J. Vaari (2004). FDS simulation of fire spread - comparison of model results with experimental data. *VTT Working Papers 4, VTT Building and Transport.*

Hu, L. H., F. Tang, D.Yang , S. Liu and R. Huo (2010). Longitudinal distributions of CO concentration and difference with temperature field in a tunnel fire smoke flow. *International Journal of Heat and* Mass Transfer 53(13), 2844-2855.

Hu, X., Z. Wang, F. Jia and E. R. Galea (2012). Numerical investigation of fires in small rail car compartments. *Journal of Fire Protection Engineering 22(4), 245-270.*

Ingason, H. (2007). Model scale railcar fire tests. *Fire Safety Journal 42(4), 271-282.*

Jia, F., E. Galea and M. K. Patel (1999). The numerical simulation of the noncharring pyrolysis process and fire development within a compartment. *Applied Mathematical Modelling* 23(8), 587-607.

Karlsson, B. and J. G. Quintiere (1999). *Enclosure fire dynamics.* CRC Press.

Kim, E., J. P. Woycheese and N. A.Dembsey (2008). Fire dynamics simulator (version 4.0) simulation for tunnel fire scenarios with forced, transient, longitudinal ventilation flows. *Fire Technology 44(2), 137-166.*

Lin, C. H., Y. M. Ferngand and W. S. Hsu (2009). Investigating the effect of computational grid sizes on the predicted characteristics of thermal radiation for a fire.*Applied Thermal Engineering 29(11), 2243-2250.*

Lemaire, T., Y. Kenyon and J. Mangs (2006). Large

scale fire tests in the second Benelux tunnel. *Fire Technology 42(4), 329-350.*

Matala, A. and S. Hostikka(2008). *Estimation of pyrolysis model parameters for solid materials using thermogravimetric data.* Fire Safety Science 9, 1213-1223

McGrattan, K. B., H. R. Baum and R. G. Rehm (1998). Large eddy simulations of smoke movement. *Fire Safety Journal 30(2): 161-178.*

McGrattan, K., S. Hostikka, J. Floyd, H. Baum, R. Rehm, W. Mell and R. McDermott (2010). *Fire Dynamics Simulator (Version 5), Technical reference guide.* NIST Special Publication 1018-5. Gaithersburg, MD, National Institute of Standards and Technology.

Moghtaderi, B., V. Novozhilov, D. Fletcher and J. H. Kent (1997). An integral model for the transient pyrolysis of solid materials. *Fire and Materials 21(1), 7-16.*

Most, J. and J. Saulnier (2011). Under-ventilated wall fire behaviour during the post-flashover period. *Journal of Applied Fluid Mechanics 4(2), 129-135.*

NIST (1999). *NIST Fire Test Database*, FASTData 1.0, National Institute of Standards and Technology, Building and Fire Research Laboratory.

Peacock, R. D. and E. Braun (1999). *Fire Safety of Passenger Trains, Phase I: Material Evaluation* (Cone Calorimeter), National Institute of Standards and Technology, Building and Fire Research Laboratory.

Peacock, R. D., P. A. Reneke, J. D. Averill, R. W. Bukowski and J. H. Klote (2002). *Fire safety on passenger trains; Phase II: Application of fire hazard analysis techniques* National Institute of Standards and Technology, Building and Fire Research Laboratory.

Peacock, R. D., J. D. Averill, D. Madrzykowski, D. Stroup, P. A. Reneke and R. W. Bukowski (2004). *Fire safety of passenger trains; Phase III: Evaluation of fire hazard analysis using full-Scale passenger rail car tests*National Institute of Standards and Technology, Building and Fire Research Laboratory.

Peters, N. (2000). *Turbulent combustion.* 1st edition. Cambridge University Press, Cambridge, UK.

Poinsot, T. and D. Veynante (2001). *Theoretical and numerical combustion. 1st edition. RT Edwards Incorporated, Philadelphia, PA.*

Rehm, R. G. and H. R. Baum (1978). The equations of motion for thermally driven, buoyant flows.*Journal of Research of the National Bureau of Standards 83(3), 297–308.*

Rockett, J. A. (1976). Fire induced gas flow in an

enclosure. *Combustion Science and Technology 12(4-6), 165-175*.

Roh, J. S., H. S. Ryou, D. H. Kimx, W. S. Jung and Y. J. Jang (2007). Critical velocity and burning rate in pool fire during longitudinal ventilation. Tunnelling and Underground Space Technology 22(3), 262-271.

Senecal, J. A. (2005). Flame extinguishing in the cup-burner by inert gases. *Fire Safety Journal 40(6), 579-591.*

Shen, D., M. X. Fang, Z. Y. Luo and K. F. Cen (2007). Modeling pyrolysis of wet wood under external heat flux. Fire Safety Journal 42(3), 210-*217.*

Shi, L. and M. Y. L. Chew (2013). A review of fire processes modeling of combustible materials under external heat flux. *Fuel 106: 30-50.*

Siegel, R. and J. R. Howell (2002). *Thermal radiation heat* transfer. 4th edition. Taylor & Francis, New York, NY.

Smagorinsky, J. (1963). General circulation experiments with the primitive equations-I. The basic experiment. *Monthly Weather Review 91(3), 99-164.*

Tewarson, A. (2002). *Generation of Heat and Chemical Compounds in Fires,* in SFPE Handbook of Fire Protection Engineerin*g, handbook of fire* protection engineering, 3[rd]edition. Quincy, Massachusetts, National Fire Protection Association.

Vaari, J., S. Hostikka, T. Sikanen and A. Paajanen (2012). *Numerical simulations on the performance of waterbased fire suppressions* systems. VTT Technology 54, VTT Technical Research Center of Finland, Espoo.

Walton, W.D. and P. H. Thomas (2002). *Estimating Temperatures in Compartment Fires, in SFPE Handbook of Fire Protection Engineering*, handbook of fire protection engineering, 3[rd]edition. Quincy, Massachusetts, National Fire Protection Association.

Wang, H. Y. (2009). Prediction of soot and carbon monoxide production in a ventilated tunnel fire by using a computer simulation. *Fire Safety Journal 44(3), 394-406.*

Yang, D., L. H. Hu, R. Huo, Y. Q. Jiang, S. Liu and F. Tang *(2011). Experimental study and* numerical simulation for a storehouse fire accident. *Building and Environment 46(7), 1445-1459.*

Zhang, X. G., Y. C. Guo, C. K. Chan and W. Y. Lin (2007). Numerical simulations on fire spread and smoke movement in an underground car park. *Building and Environment 42(10), 3466-3475.*